DESIGN AND OPTIMIZATION OF COMPOSITE LAMINATES REPAIRED BY BONDING EXTERNAL PATCHES

P. Cheng, X.J. Gong*, S. Aivazzadeh
Laboratory LRMA-DRIVE, ISAT, University of Burgundy, Nevers, France
* Corresponding author (xiao-jing.gong@u-bourgogne.fr)

Keywords: *composite laminates, repair, patch, optimization, finite element analysis*

Abstract
The present study proposes a design tool for optimizing external patched repairs. Damage development and the failure process of the repaired plates were analyzed. It was found that high stress concentration along the transverse edges of circular patches and/or at the longitudinal edges of the hole leads to early damage initiation in the parent plate. It is shown that the damage progression depends on the repair patch. This study considered various patches of different stacking sequences placed on both sides of the parent plate. Finite element analysis was used to optimize patched repairs. The optimized patch design can be characterized by an optimal strength ratio R*, and a parameter K has been proposed for the patched repair optimization.

1. Introduction

The increased use of composite structures in the transport industry pose questions about the repair of damaged composites structures. In large applications the composite elements partially damaged by low-speed impacts will have reduced mechanical performance. In many cases, the cost of complex composite structures is too high to systematically replace damaged ones. A local repair can be considered as a good solution for economical and mechanical reasons and one of the repair methods frequently used by industry consists in bonding composite patches to the damaged areas [1-5]. Design and optimization of this type of repair have been shown to be very complex [6-9].
This study proposes a design tool for optimizing external patched repairs. Experimental observations associated with finite element analysis have shown that measured failure load varies in the same tendency as that of calculated damage initiation as a function of different repair parameters. An optimal strength ratio R* has been defined. Finally, a parameter K has been proposed for the purpose of patched repair optimization.

2. Experimental details

The parent composite plates were laid up to give a quasi-isotropic structure with the following stacking sequence: [45/-45/0/90]s. Patches were made from the same material but with stacking varying sequences. A toughened single part epoxy adhesive was used with a controlled 0.2 mm thick bond line (*MASTERBOND ESP 110*). Material properties are presented in Table 1. The configuration of repaired test specimens is shown in Figure 1. The 10 mm diameter hole in the parent plate is to simulate a damaged zone. The circular patches, cut from plate material, are bonded symmetrically to each side of the specimen using standard bonding procedure. In practical terms the holes are filled with adhesive. Glass/epoxy tabs are bonded to the specimens in the grip area. The tensile tests were run at room temperature on an MTS DY-36 universal test machine fitted with a 100 KN load cell. Load speed was 0.5 mm/min and at least five specimens were tested in each configuration.
Specimens were divided into two series so as to more clearly understand the factors impacting on repair behaviour. Series I patches are designed to vary the in-plane stiffness over a wide range. These characteristics are shown in Table 2 where A_{11} refers to the in-plane stiffness in the loading direction and *h* is patch thickness. It should be noted that the fibre angle of the patch lay-up in contact with the parent plate also varies with the stacking sequence. For Series II patches the ratio A_{11}/h was held constant but stacking sequences were changed in order to

determine the importance of this variable on the performance of repaired systems [7-9].

3. Finite element analysis

A 3-D finite element analysis using MSC.Patran with a Marc 2005 solver was carried out to determine stress/strain distribution in the patches and parent plates.

Due to symmetry considerations, only one half of the repaired test specimen is modelled in the FEA (Figure 2). Boundary conditions are simulated by fixing one end and applying a constant displacement in the longitudinal direction at the other. It was confirmed that the constant displacement gives rise to a constant reaction at the boundary since the repaired zone is sufficiently far from the fixed end. The adhesive bondline is simulated as being isotropic with elastic-perfectly plastic behaviour. Elastic behaviour for the composite is assumed. The patches and the parent plate are meshed using the real stacking sequences with hexahedron 20-node brick elements. Convergence testing was performed in high stress concentration areas. A 9384-element mesh model was adopted because it proved to accurately describe the damage initiation zones observed in the test specimens and was applied to all the repair configurations. In this study, static strength analysis only was performed.

4. Results and discussions

4.1 Failure process of parent plate

- *Fracture surface observation*

The fracture surfaces were examined by low magnification photography in order to describe the failure mechanisms of patched repairs. For specimens having Series I-2 patches (Table 2), Figure 3-a is typical of this failure type: a large amount of fibre breakage and delamination can be seen near the edge A of the patch, patches are partially or even completely separated from the parent plate and also have broken fibres attached to them. This implies that the parent plate ply adjacent to the adhesive is particularly damaged and delaminated before specimen failure. The repairs using stiff patches $[0]_4$ showed similar failure surface.

In the case of the repairs using Series I-1 patches, which have the lowest value of A_{11}, the fracture surface were considerably different from the previous examples as can be seen in Figure 3-b, but in fact very similar to that of notched specimens without repair. Here the fracture surface in the plane perpendicular to the load direction is located in the section weakened by the hole. Signs of delamination and fibre breakage are much less visible near the patch edge A. So damage is suggested to initiate at the edges of the hole in the parent material, noted as C. In this case, rapid damage growth leads to the final failure along the transverse direction through the hole.

- *Damage detection by acoustic emission*

In order to locate damage initiation and follow the damage propagation during tension testing, three acoustic emission sensors with diameter of 10 mm were placed on the patches and on the parent plate of the repairs using different patches. The Figure 4-a shows schematically the position and numbering of acoustic emission sensors on all our repairs tested. The choice of the position of three sensors on the repaired specimen results from many tests.

The signals recorded during the tests are processed using different parameters. After many tests it appears that the accumulated energy is the best candidate to detect damage initiation.

An example is given in Figure 4, where the specimen is repaired by patches $[0]_4$. It is indicated that damage initiation occurs at the longitudinal ends of the patches, defined as Zone A. Damages are also formed at the edge of the hole in zone C (Image (b)). The image (c) shows that the spread of the damaged area in Zone A runs symmetrically inward patches. It should be accompanied by the delamination in the parent plate and then fiber breakage because the output of the accumulated energy looks high. The image (d) suggests that the patches have already partially or completely detached from the plate before the final failure. Fiber breakage in the critical section around the hole leads to the final failure of the repaired specimen.

For others repairs, it is shown that the acoustic emission is also very efficient to locate damage initiation and follow damage propagation.

- *Other experimental methods*

Other experimental observations were described in a previous work [9], such as:

- Loading vs. displacement curves
- Infrared thermography
- Strain gauges

These observations were necessary to validate the finite element analysis model.

4.2 Optimization parameter

In our finite element analysis, both Tsai-Wu and Hoffman failure criteria were used to predict damage initiation of the repair systems. Although these criteria cannot give the real damage mode they can take into account the interactions between different stresses. It was found that the results obtained using these criteria were virtually the same, so in the remainder of the discussion only results pertaining to the Hoffman criterion will be considered, namely, in terms of the strength ratio R as defined by Equation 1.

$$R=C_1(\sigma_2-\sigma_3)^2+C_2(\sigma_3-\sigma_1)^2+C_3(\sigma_1-\sigma_2)^2+C_4\sigma_1+C_5\sigma_2+C_6\sigma_3+C_7\sigma_{23}^2+C_8\sigma_{13}^2+C_9\sigma_{12}^2 \quad (1)$$

Where:

$$C_1=\frac{1}{2}\left(\frac{1}{Z_tZ_c}+\frac{1}{Y_tY_c}-\frac{1}{X_tX_c}\right)$$

$$C_2=\frac{1}{2}\left(\frac{1}{X_tX_c}+\frac{1}{Z_tZ_c}-\frac{1}{Y_tY_c}\right)$$

$$C_3=\frac{1}{2}\left(\frac{1}{X_tX_c}+\frac{1}{Y_tY_c}-\frac{1}{Z_tZ_c}\right)$$

$$C_4=\frac{1}{X_t}-\frac{1}{X_c} \qquad C_5=\frac{1}{Y_t}-\frac{1}{Y_c} \qquad C_6=\frac{1}{Z_t}-\frac{1}{Z_c}$$

$$C_7=\frac{1}{S_{23}^2} \qquad C_8=\frac{1}{S_{13}^2} \qquad C_9=\frac{1}{S_{12}^2}$$

If $|R|\geq 1$, damage will occur.

For the adhesive joint, critical plastic strain criterion is applied to predict its failure.

The finite element analysis is carried out by applying a uniform displacement of 0.5 mm at one end of the half specimen model (corresponding to a 1 mm displacement for the whole specimen) which remains within the elastic domain of the composite material.

It is evident that the performance of composite structure depends on the R-distribution. The high performance of a repaired system can be attained if maximal value of R value in the parent plate, defined as $R_{max\text{-}parent\ plate}$, is lowest. In general four possible critical zones in a patch repaired system can be identified (Figure 5):

- zone A: at the transverse edges of the patch
- zone B: at the transverse edges of the hole
- zone C: at the longitudinal edges of the hole
- zone D: at the longitudinal edges of the patch

If each patch A_{11}* value is normalised by that of the parent plate and the maximum R values of each potential critical zone ($R_{max\text{-}zone\ A,\ B,\ C\ \&\ D}$) of a repaired specimen are normalised by the maximum R value of the unnotched specimen, we can study their relation and variation in Figure 6 to understand the role of the patches on the system behaviour.

It can be seen that zones A and C are systematically more loaded, although the relative strength ratio in zone A increases but decreases in zone C with increasing normalised stiffness ratio (A_{11}*-patch/A_{11}*-parent plate). For the specimens repaired with [45/-45]s patches it was expected that failure should initiate in the section of the specimen weakened by the presence of the hole that includes zone C whereas for other patch types damage should start from zone A. These conclusions are really confirmed by the observations on tested specimens. It can be deduced that the intersection of these two curves, where $R_{max\text{-}zone\ A}$ is equal to $R_{max\text{-}zone\ C}$, should give the best performance of repairs. The value of R at this point is defined as R*.

Assuming $\alpha = 1/R_{max\text{-}parent\ plate}$, it can be in fact used to describe the effectiveness of a repair. Figure 7 compares the parameter α obtained by finite element analysis with the normalised failure load measured by experimentation. It is interesting to see that the evolution of theses two parameters as a function of the normalised patch's stiffness is following the same tendency. It can be concluded that the parameter α or $R_{max\text{-}parent\ plate}$ is an indicator of the performance of repaired systems.

Consequently, the optimisation of the patch repaired system consists in varying different repair parameters in order to maximize α or minimise

$R_{max\text{-}parent\ plate}$. Some repair parameters were analyzed one by one in reference 8 [8], such as: patch stacking sequences; patch thickness (t_p); adhesive thickness (t_a) and Young's modulus of adhesive (E_a).

4.3 Design parameter *K*

In order to understand the interaction between the different parameters of a patched repair, the results obtained are compared in Figure 8. The relationship between these parameters looks complicated. In reality, for a real repair system en composite, some specific requirements have to be considered, such as adhesive proprieties, patch and bonded joint geometry, etc. So the repair parameters can be chosen in a limited range. If some parameters are already selected, we need to know how to optimize other parameters. For the purpose of design, we propose a dimensionless parameter K, which will be able not only to integrate the effect of different repair parameters in a simple manner, but also to be determined easily. Equation 2 is proposed according to the results obtained by finite element analyses and experimental tests.

$$K = \alpha \left(\frac{E_a}{t_a} \frac{t_p}{E_p} \right)^{\beta} \frac{E_p t_p}{E_{pp} t_{pp}} \qquad (2)$$

Where:

- E_a and t_a are Young's modulus and thickness of adhesive;
- E_p and t_p are Young's modulus in loading direction and thickness of patch;
- E_{pp} and t_{pp} are Young's modulus in loading direction and thickness of parent plate;
- α and β are repaired structure coefficients. They have to be determined empirically/ numerically.

The use of this parameter supposes that if:

- K = 0, no repair ($R_{zone\ C} >> R_{zone\ A}$)
- 0<K<1, insufficient repair ($R_{zone\ C} > R_{zone\ A}$)
- K = 1, optimal repair ($R_{zone\ C} = R_{zone\ A}$)
- K>1, excessive repair ($R_{zone\ C} < R_{zone\ A}$)

In the case of the circular patch repair stressed in tension, it was obtained: $\alpha \approx 6.12$ and $\beta \approx 0.25$.

In attention to establish a more general model of design assistance, the model of K (equation 2) can be generalized to take into account more repair parameters. Equation 3 is so proposed including all types of reinforcements. The first term reflects the effect of the repair plug or by "internal" patch and the second term the effect of the repair by "external" patches:

$$K = \lambda \psi \left(E_b, E_{pp}, E_a, t_a, L_b \ldots \right) + \alpha \left(\frac{E_a t_p}{E_p t_a} \right)^{1/4} \frac{E_p t_p}{E_{pp} t_{pp}} \qquad (3)$$

Where:

- α and λ are two repair constants to be adjusted empirically and/or experimentally.
- ψ is a function that translates the effects of the rigidity of parent plate, the internal patch and adhesive between the patch and the hole, the geometry of the internal patch Lb (scarf, cylindrical, etc ...) and thickness of the bonded joint can also affect the repair performance.

In reality the validation of such models requires much more experimental and numerical results.

5. Conclusions

The acoustic emission is shown very efficient to locate damage initiation and to follow damage propagation in a repaired system.

Experimental observations associated with finite element analysis have shown that measured failure load varies in the same tendency as that of calculated damage initiation as a function of different repair parameters.

It has been possible to define a strength ratio R* that is key in defining an optimal patch design for a parent material; repair parameters should be chosen to minimise the R* value.

The effects of several parameters on the performance of the repairs, such as Young's modulus and the thickness of adhesive, the stiffness and the thickness of patch, can be integrated into a dimensionless design parameter K. This type of model can be generalized to the internal or/and external patches. Much more experimental work is needed to propose a final form of the model and to validate it.

Table 1: Mechanical properties of materials

Material	T600S/R368-1	ESP 110
E1 (GPa)	103	3
E2, E3 (GPa)	7	
ν12	0.34	0.3
ν23	0.30	
ν31	0.023	
G12, G13 (GPa)	3.15	
G23 (GPa)	2.75	
Xt (MPa)	2006	
Xc (MPa)	1500	
Yt, Zt (MPa)	44	
Yc, Zc (MPa)	140	
S12, S13 (MPa)	65	40
S23 (MPa)	32.5	

Table 2: Series I patch characteristics

No.	Stacking sequence*	A_{11}* =A11/h (GPa)
I-1	$[45/-45]_s$	11.4
I-2	[90/0/-45/45]	39.2
I-3	$[0]_4$	103.0

** The first layer is in contact with the adhesive*

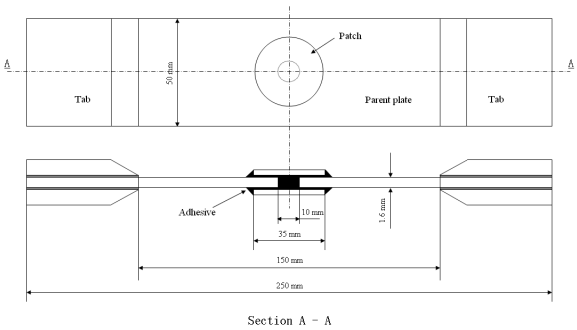

Fig. 1. Repaired test specimens

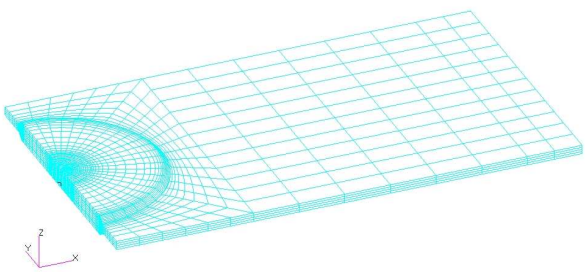

Fig. 2. Mesh model: half specimen

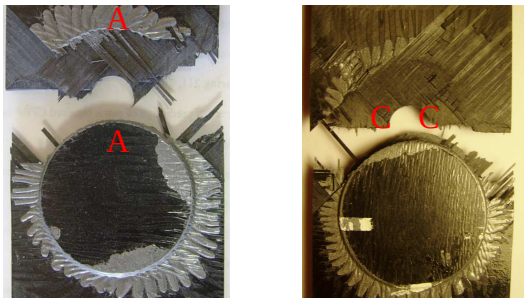

(a) [90/0/-45/45] (b) $[45/-45]_s$

Fig. 3. Failure in the repaired specimens

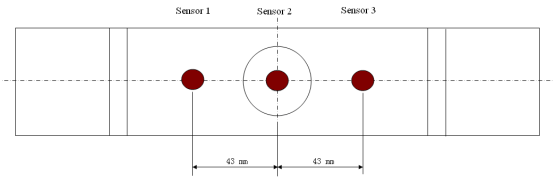

(a) Position and numbering of three AE sensors

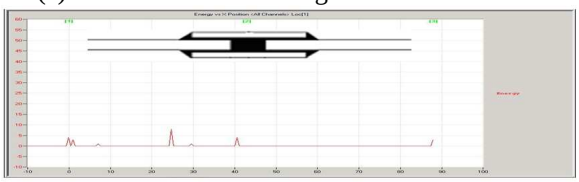

(b) Image of acoustic mission at 20% failure loading

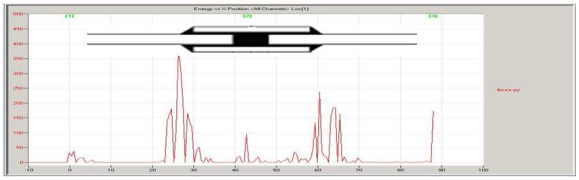

(c) Image of acoustic mission at 65% failure loading

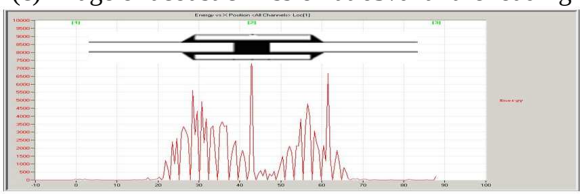

(d) Image of acoustic mission at 100% failure loading

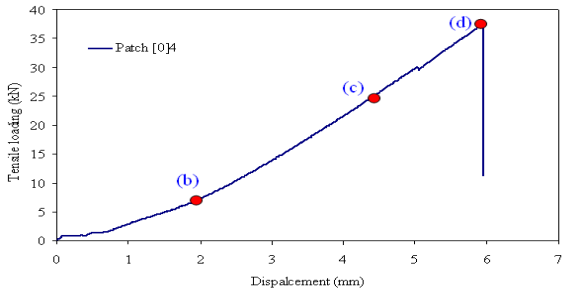

(e)

Fig. 4. Control with acoustic emission on a specimen repaired by patchs $[0]_4$

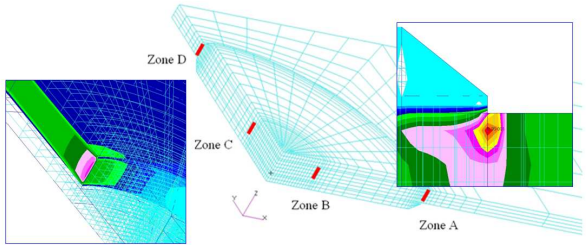

Fig. 5. Location of the 4 possible critical zones in a patch repaired system

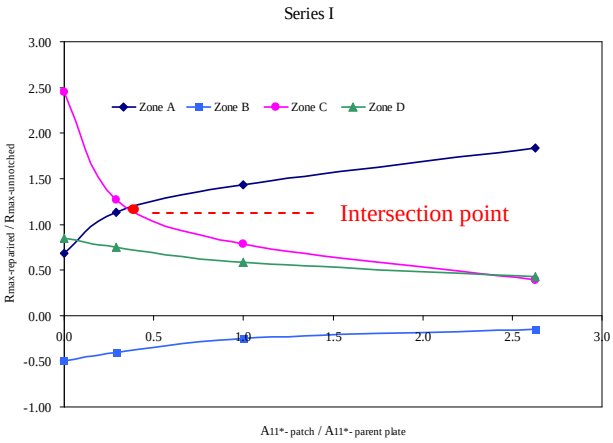

Fig. 6. Maximal strength ratio R in zones A, B, C and D as a function of A_{11}* (normalized) in the load direction of the studied patches in series I

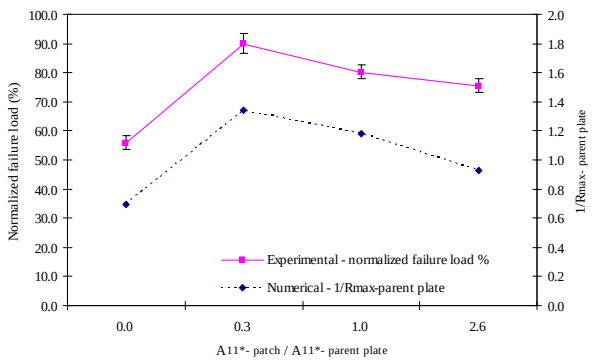

Fig. 7. Normalized failure load measured on the specimens repaired by patches in series I and the prediction of the damage initiation by FEA

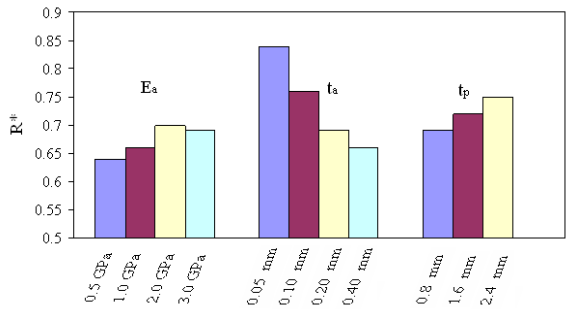

Fig. 8. Variation of R* vs. different parameters

References

[1] C. Soutis and F. Z. Hu. "Design and performance of bonded patch repairs of composite structure". *Proc Instn Mech Engrs* Vol 211 Part G, 1997.

[2] F. Z. Hu and C. Soutis. "Strength prediction of patch-repaired CFRP laminates loaded in compression". *Composites Science and Technology*, 60 (2000) 1103-1114.

[3] C. Soutis, D. M. Duan and P. Goutas. "Compressive behaviour of CFRP laminates repaired with adhesively bonded external patches". *Composite Structures*, 45 (1999) 289-301.

[4] J. Rodes, R. Brossier, X.J. Gong and J. Rousseau. "Etude des performances des structures composites réparées". *Matériaux*, 13-17 Novembre2006, Dijon, France

[5] X. Liu and G. Wang. "Progressive failure analysis of bonded composite repairs". *Compsite Structures*, 81 (2007) 331-340

[6] P. Cheng, X.J. Gong, Rousseau and S. Aivazzadeh. "Optimisation des patchs de réparation des structures composites". *Journées Nationales sur les Composites*, 6 au 8 juin 2007, Marseille, France

[7] X.J. Gong, P. Cheng, J. Rousseau and S. Aivazzadeh. "Effect of local stresses on static strength and fatigue life of patched composite panels". *16th International Conference on Composite Materials*, 8-13 July 2007, Kyoto, Japan

[8] P. Cheng, X.J. Gong and S. Aivazzadeh. "Optimization of patched repair for CFRP laminates". *17th International Conference on Composite Materials*, 27-31 July 2007, Edinburgh, UK

[9] P. Cheng, X.J. Gong, D. Hearn and S. Aivazzadeh. "Tension behaviour of patch-repaired CFRP laminates". *Composite structures*, 93 (2011) 582-589